Original Article

Iraqi National Journal of Medicine. July 2025, Volume 7, Issue 2

Evaluation of anatomic and dosimetric changes during simultaneously integrated boost volumetric modulated arc therapy for head and neck cancer

Farah Dirar Yousif [1], Raad Hefdhi Abedtwfeq [2]

[1] Baghdad radiation oncology and nuclear medicine hospital, Baghdad medical city, Baghdad, Iraq. [2] Department of radiology, Al-Yarmuk teaching hospital, Baghdad, Iraq.

ABSTRACT

Background: Volumetric modulated arc therapy (VMAT) is the most commonly used radiotherapy (RT) technique for locally advanced head and neck cancers (HNC), concurrent with chemotherapy. **Aim**: This study aims to evaluate the anatomical changes that may arise in patients undergoing VMAT treatment. **Methods**: The study involved 20 patients with locally advanced HNC who received VMAT treatment concurrently with chemotherapy. Prior to the initiation of radiotherapy treatment, computed tomography (CT) simulation was conducted for all patients. The prescribed doses for the primary target (PTVP), high-risk lymph nodes (PTV60), and low-risk lymph nodes (PTV54) were 69.96 Gy, 60 Gy, and 54 Gy, respectively, administered in 33 treatment fractions using the simultaneous integrated boost (SIB) technique. Anatomical comparisons were made between CT1, CT2, and CT3, while dosimetric evaluations were performed between iplan, Rplan1, and Rplan2. **Results**: The analysis revealed a significant weight decrement in terms of anatomical changes in all patients. The gross tumor volume (GTV) decreased notably at CT2 in comparison to CT1. The GTV volume decreased significantly again at CT3. Additionally, there was a substantial reduction in the volume of the parotid glands. For dosimetric evaluation, most organs at risk experienced a noteworthy increase in the received dose. For target coverage, the D95% of the PTVP in the (iplan) was 97%, which significantly increased in Rplan1. **Conclusion**: Patients with HNC must undergo a new CT simulation during the RT course owing to significant anatomic changes that impact the plan quality. New plans (adaptive plans) should be implemented for a specific number of fractions to ensure the maintenance of initial plan quality.

Keywords: adaptive radiotherapy, head and neck cancers, IMRT, VMAT, radiotherapy

Corresponding author: Farah Dirar Yousif. E-mail: joym7131@gmail.com
Disclaimer: The authors have no conflict of interest.

DOI: https://doi.org/10.37319/iqnjm.7.2.7

Received: 7 MAR 2025 Accepted: 23 APR 2025 Published online: 15 JUL 2025

INTRODUCTION

The incidence of cancer is on the rise in different communities, making it the second leading cause of death in developed countries.[1] Head and neck cancers (HNC) constitute 2 to 5% of these malignancies, representing a heterogeneous group of neoplasms originating from the oral cavity, oropharynx, hypopharynx, larynx, and other areas.[2] Radiotherapy (RT), along with chemotherapy and surgery, is one of the

main modalities in the management of cancer. The goal of RT is to provide maximum damage to tumors while minimizing damage to surrounding the healthy tissues.[3]

HNC accounts for approximately 4% of all cancer cases, presenting a variety of neoplasms with diverse natural histories arising in the relatively small region of the head and neck.[4] Depending on the site, size, and pattern of spread, HNC can cause various degrees of structural deformities and functional handicaps, compromising comfort and social integration, including in thyroid disorders.[4,5] Integrated interdisciplinary collaborations among surgical, radiation, medical, and dental oncologists, as well as interactions among oncologists, pathologists, radiologists, reconstructive surgeons, physical medicine and rehabilitation physicians, psychiatrists, nurses, speech and swallowing therapists, dietitians, social workers, chaplains, and other health and spiritual care personnel are essential for the optimal management and rehabilitation of patients with HNC.[4] Well-functioning, integrated, and coordinated care is imperative in achieving the highest complication-free cure rate with maximal functional and cosmetic outcomes.[6]

Patients with HNC are characterized by a moderate overall prognosis and relatively poor compliance, leading to frequent loss of follow-up sessions.[2]

Radiotherapy (RT) plays a crucial role in the treatment of head and neck squamous cell carcinoma (HNSCC), often involving modern RT techniques that use modulated radiation intensities. These techniques allow dose elevation in tumor volume and offer better sparing of the organs at risk (OAR). Although intensity-modulated radiation therapy (IMRT) and volumetric modulated arc therapy (VMAT) are now standard treatments in most centers worldwide, they produce steep dose gradients, which means that any minimal changes in patient anatomy, tumor volume, and OAR position can compromise the coverage of the target volumes and lead to an overdose of critical and normal structures.[7]

Throughout the course of RT for HNC, anatomical changes may occur from the first irradiation sessions, including the reduction of the tumor and even normal tissues, leading to organ movement and position changes relative to other structures. Weight loss in patients with HNC is very common due to swallowing difficulties that can be caused by either the size of the tumor that prevents swallowing or the side effects induced by RT and chemotherapy. A quantification of weight loss among HNC patients was reported by Ho et al., revealing a 7.6% decline in weight throughout course of treatment [8]. In the same context, Bhandari et al. reported a 10% weight loss after the third week of RT.[8,9]

The tumor volume drop during HNC RT was demonstrated by Burela et al., who showed that the reduction in the planning target volume (PTV) after four weeks of RT was 13.16%, whereas the parotid glands decreased in volume by 27.31% and 24.63%, respectively.[10] These anatomical changes can have a significant impact on treatment outcomes, as even small shifts in the patient's anatomy and tumor position can lead to significant dosimetric changes. This causes complications during treatment owing to the overdose of some sites or marginal recurrences owing to an underdose of the target volume. To minimize these effects during RT, one potential strategy is adaptive radiation therapy (ART), which involves conducting computed tomography (CT) rescans of the patient and making adjustments to the treatment plan based on the new anatomy of the patient.[10]

Buciuman and Marcu[11] concluded that the VMAT technique combined with ART counteracted anatomical changes during HNSCC treatment. ART is a treatment technique that can systematically improve treatment plans in response to patient/organ temporal variations observed during RT.

Recently, magnetic resonance imaging (MRI) guided RT has been evaluated for its utility in Arc-Adaptive radiation therapy (A-ART),[12,13] with the idea that adaptive scans utilizing MRI can dramatically improve the visualization of soft tissue changes throughout treatment.[14]

Our study investigated the impact of anatomical changes in patients during a RT course on the quality of volumetric-modulated RT plans for HNC. Additionally, offline adaptive planning was applied to evaluate dosimetric outcomes in the cases.

MATERTIALS AND METHODS

Patient Characteristics

This prospective study was conducted at the Baghdad Center for Nuclear Medicine and Radiotherapy and the Al-Andalus Oncology Center between October 2022 and October 2023.

The study included 20 patients with locally advanced HNC with the following primary tumors: 10 nasopharyngeal carcinomas, six maxillae, and four oropharyngeal carcinomas. Table 1 presents the patient characteristics (inclusion criteria) in detail.

Table 1: Patient's characteristics (N=20)

Characteristic	No. of patients (%)
Age (yr.)	
≤ 50	5 (25)
> 50	15 (75)
Sex	
Male	13 (65)
Female	7 (35)
Primary site	
Maxilla	6 (30)
Nasopharynx	10 (50)
Oropharynx	4 (20)
Clinical T stage	
T1	3(15)
T2	5 (25)
T3	10 (50)
T4	2 (10)
Clinical N stage	
N0	2 (10)
N1	4 (20)
N2	8 (40)
N3	6 (30)
Concurrent chemoradiation	
No	0 (0)
Yes	20 (100)

Patients with metastatic HNC were excluded. All the patients consented to participate in the study.

Dose Prescription

As previously mentioned, all patients were diagnosed with locally advanced HNC and underwent chemotherapy concurrent with RT. The prescribed RT doses were 70 Gy for the primary target (PTVP), 60 Gy for the high-risk lymph nodes (PTV60), and 54 Gy for the low-risk lymph nodes (PTV54). All doses were administered in 33 treatment sessions using the simultaneous integrated boost (SIB) technique.

Patient's Imaging, Contouring, and Planning

For the best clinical outcomes, all patients in this study underwent MRI and positron emission tomography (PET) to ensure gross tumor volume (GTV) location and size precision. Moreover, patients underwent CT simulation to prepare for RT treatment, where computed tomography (CT) (GE revolution EVO, GE health care, JAPAN Corporation) was used with a slice thickness of 2.5 mm for better dose calculation. The CT images were then exported to the Monaco treatment planning system (Monaco version 5.1.1), where contouring of organs at risk and targets was performed on the acquired CT images using the latest guidelines.[15,16] After contouring, a VMAT plan was achieved by the physicist using the SIB technique for all cases, where the doses to the target and OARs were calculated and approved by the radiation oncologist. When 10 treatment fractions were completed, a new CT simulation was performed (CT2), and the original VMAT plan with the same parameters and constraints was projected on the new CT study and called registered plan1 (Rplan1). After another 10 fractions (after 20 treatment sessions), patients acquired a new CT simulation (CT3), and the original VMAT plan was again projected on CT3 and called registered plan2 (Rplan2). In contrast, a new plan with new constraints was executed on CT2 and called adaptive replan 1 (ARplan1). In addition, a new plan was achieved in CT3, adhering to the latest guidelines and constraints.

Anatomic and Dosimetric Assessment

The anatomical evaluation includes measuring and comparing the volumes of the gross tumor (GTV) and parotid glands between CT1, CT2, and CT3. In addition, the patient's weight was measured and compared between CTs scans. For the dosimetric outcomes, the doses received by OAR and targets were calculated and compared between the initial plan (iplan), Rplan1, and Rplan2. Furthermore, the dosimetric outcomes were compared between the original plan, ARplan1, and ARplan2.

The conformity index (CI), one of the qualitative tools used to evaluate the target coverage and how much the dose is conformed around the target, and heterogeneity index (HI), another qualitative tool for plan evaluation that is used to measure the homogeneity of the dose inside the target, were calculated and compared between initial, registered, and adaptive plans. The CI was calculated using the van't Riet et al. formula.[17]

$CI = (TV_{RI})^2 / (TV * V_{RI})$

where CI is the conformity index, TV_{RI} is the target volume covered by the reference dose, TV is the target volume, and V_{RI} is the reference dose volume.

The HI was calculated using the formula presented by Semerenko et al.[18]

$HI = D_{5\%} / D_{95\%}$

where the HI is the heterogeneity index, $D_{5\%}$ is the maximum dose received to 5% of the target volume, and $D_{95\%}$ is the minimum dose received to 95% of the target.

Statistical Analysis

The Wilcoxon signed-rank test was used to compare two variables, with a change deemed significant if the P-value was less than 0.05.

Ethical Clearance

By Baghdad Radiation Oncology and Nuclear Medicine Hospital, Baghdad Medical City (no. 203 in 10 Sep 2022).

RESULTS

Anatomical Changes

Following the administration of chemotherapy combined with RT, a notable reduction in tumor volume was observed. The median GTV_P prior to treatment (GTV1) was 25[18.2–56.3] cc, and interestingly ($p < 0.001$), the volume fell to 20[15–47] cc after 10 RT treatment fractions (GTV2). The tumor response continued after 20 fractions (GTV3), where the GTV was reduced significantly to reach 17[10–41] cc. Figure 1a demonstrates the change in tumor volume during the RT sessions. Another effect of radiation on the human anatomy observed during the course of RT was the change in parotid gland volume, where a part of the parotids was located inside the radiation field because of its proximity to the target area. A significant reduction in left parotid gland volume was observed after 10 treatment fractions, where the mean left parotid volume at CT1 was 27[21–38] cc and then decreased to 23[14–31] at CT2 ($p < 0.001$). At CT3, the left parotid volume decreased to 16[11–27] cc. Figure (1b) depicts the changes in left parotid volume during the RT course. With the same pattern, the right parotid gland was significantly reduced, and the parotid gland volume recorded a median volume of 28[18–41] cc, 22[12–32] cc, and 16[11–28] cc at CT1, CT2, and CT3, respectively (Figure 1c).

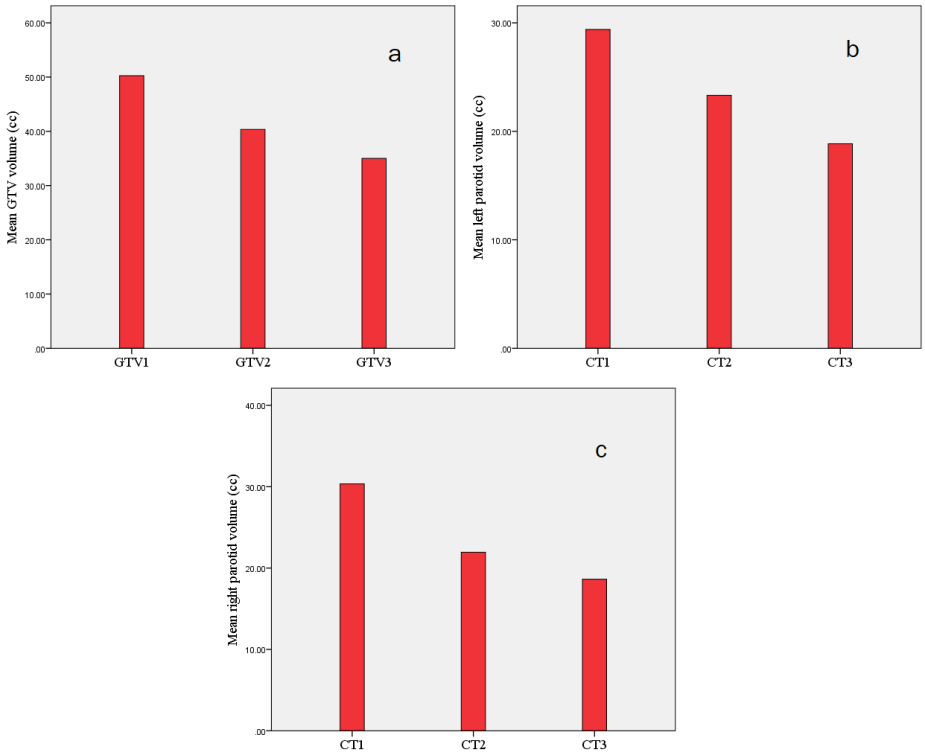

Figure 1: a. GTV volume changes during radiotherapy course; b. Left parotid volume changes during the radiotherapy course; c. Right parotid volume changes during the radiotherapy course.

The volume of PTV_P also experienced a reduction due to GTV reduction The PTV_P before RT sessions was 115[67–173] cc, and a significant reduction in volume was seen at CT2 ($p = 0.001$) at CT2 with a value of 97[47–148] cc. The change in parotid volume is clearly illustrated in Figure 2. The PTV_P was also significantly decreased at CT3 compared to that at CT2 ($p = 0.001$), where the median volume at CT3 was 82[33–136] cc. Figure 2 gives us a clear image of the primary target volume changes during the RT course.

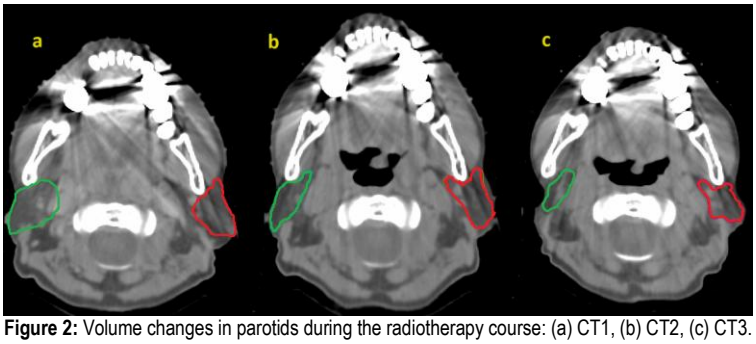

Figure 2: Volume changes in parotids during the radiotherapy course: (a) CT1, (b) CT2, (c) CT3.

In addition to achieving the primary target volume reduction, the high- and low-risk target volumes were substantially reduced during RT. For high-risk target volume (PTV_{60}), the initial median volume at CT1 was 374[257–517] cc, with significant reduction in volume observed (p = 0.001) at CT2 with a median volume of 332[213–416] cc. Moreover, the PTV_{60} volume also significantly decreased at CT3 compared to CT2, where the median volume reached 299[196–392] cc, as clearly seen in Figure 3a. For the low-risk target (PTV54), the median volume at CT1 was 423[321–623] cc. A significant reduction in volume was observed at CT2 ($p < 0.001$) in comparison to CT1, where the volume was 385[265–585] cc, Figure 3b. Furthermore, the PTV_{54} median volume significantly decreased at CT3 compared to CT3, with a volume equal to 361[231–452] cc. Figure 3c represents the change in PTV_{54} volume through the RT fractions.

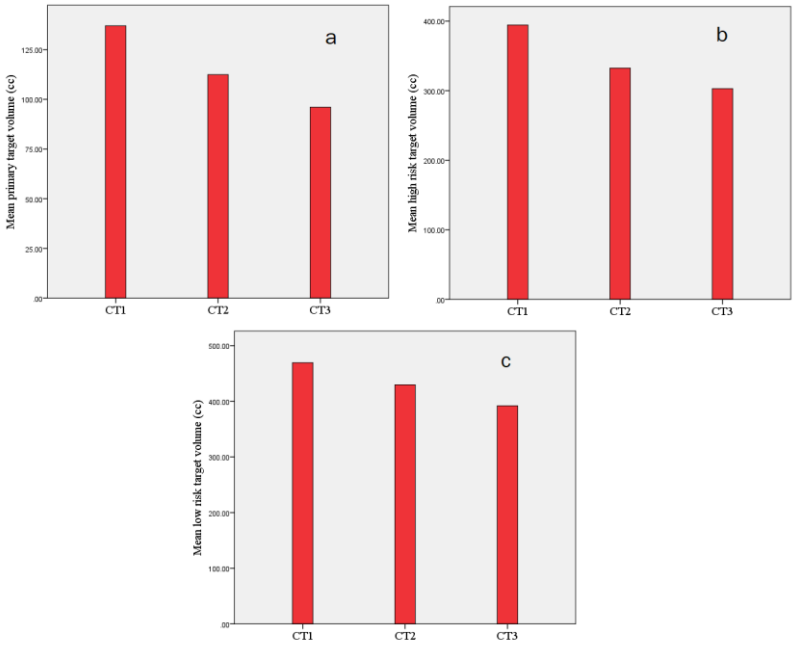

Figure 3: a. PTVP volume changes during radiotherapy course; b. PTV60 volume changes during radiotherapy course; c. PTV54 volume changes during radiotherapy course.

Throughout the RT course, a notable anatomic change was observed in the weight of the patients, with all patients showing a significant decrease in weight during VMAT sessions. The median weight of patients at CT1 was 77[65–89] Kg, which reduced significantly ($p < 0.001$) to 76[64–88] Kg at CT2, and further reduced at CT3 ($p < 0.001$) to 75[63–85] Kg, as shown in Figure 4.

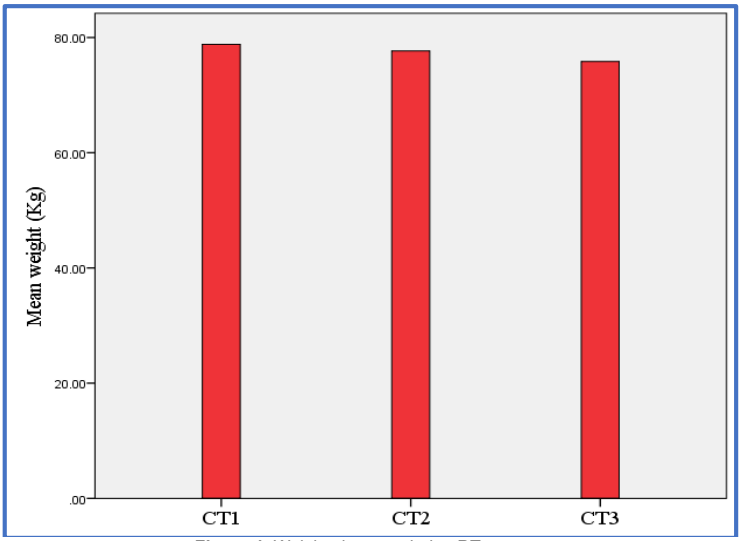

Figure 4: Weight changes during RT course.

Dosimetric Changes

Dose evaluation for organs at risk

As we saw in the previous section, there were significant changes in HNC patients during the RT course, including tumor and parotid gland volume reduction and weight loss, which may affect the quality of the approved plan. Therefore, in this section, we investigate the effect of using the same VMAT plan throughout the RT course on the dose delivered to healthy organs and targets.

Analyzing the OAR individually, the median maximum dose to the brainstem in the iplan was 4920[4472–5322] cGy, which remained relatively unchanged ($p = 0.23$) after 10 fractions (Rplan1) to reach 4885[4457–5419] cGy (noting that the maximum dose increased in the cases where the brainstem was close to the target). Following 20 sessions (at Rplan2), the median maximum dose of the brainstem significantly rose ($p = 0.006$) compared to that of the iplan and Rplan1, where it reached 5150[4580–5846] cGy. For the spinal cord at the iplan, the median maximum dose was 4015[3790–4222] cGy, and a significant rise ($p < 0.001$) occurred at Rplan1, with a value equal to 4272[4030–4574] cGy. The median maximum dose significantly increased again ($p = 0.001$) at Rplan2 reaching 4574[4161–4961] cGy. The mandible exhibited an insignificant increase ($p = 0.9$) in maximum dose at Rplan1 in comparison with iplan, where the values at the maximum dose were 6536[6311–7065] cGy and 6592[6222–7138] cGy at Rplan2 (again, the noticeable increase in dose was at a location near the target). The increment in dose was also deemed insignificant ($p = 0.890$) for Rplan2 compared to Rplan1, with a median maximum dose of 6600[6209–7239] cGy.

With respect to optical structures, the optic chiasm showed a significant dose increment at Rplan1 ($p = 0.04$), with a median maximum dose of 4370[3790–4850] cGy, from 4250[3743–4788] cGy at the iplan. The maximum dose then increased significantly ($p < 0.001$) at Rplan2, with a median value of 4650[3810–5208]. Additionally, the left optic nerve presented a notable increase ($p = 0.001$) in maximum dose at Rplan1 from the iplan, where the median maximum dose at the maximum dose was 4240[3349–5024] cGy and 4281[3401–5107] cGy at Rplan1. The dose increased significantly in Rplan2 ($p < 0.001$), with a median maximum dose of 4395[3553–5345] cGy. Consider another example of an optic structure, the left eye. The left eye median maximum dose was insignificantly increased ($p = 0.13$) at Rplan1 compared to that at the iplan, where the median maximum doses were 339[266–612] cGy and 354[269–571] cGy at iplan and Rplan1, respectively. In addition, the median maximum dose increased insignificantly ($p = 0.8$) at Rplan2 360[258–653] cGy. For the parotid glands, the median mean dose was significantly increased after 10 fractions ($p < 0.001$), with a value of 2428[2176–2603] cGy compared to 2121[1960–2228] cGy at the iplan. After 20 fractions, the median mean dose to the left parotid increased again ($p < 0.001$) to 2871[2311–3360] cGy as. Table 2 briefly describes the dose received by the organs at risk in the iplan, Rplan1, and Rplan2.

Table 2: Dose change for OAR at iplan, Rplan1, and Rplan2.

End Point median[25th, 75th] Gy	iplan	Rplan1	P value (iplan vs. Rplan1)	Rplan2	P value (Rplan1 vs. Rplan2)
Brainstem max dose	49.2[44.7–53.2]	48.9[44.6–54.2]	0.23	51.5[45.8–58.5]	0.006
Spinal cord max dose	40.2[34.9–42.2]	42.7[40.3–45.7]	< 0.001	45.7[41.6–49.6]	0.001
Mandible max dose	65.4[63.1–70.1]	65.9[62.2–71.4]	0.9	66 [62.1–72.4]	0.89
Optic chiasm max dose	42.5[37.4–47.9]	43.7[37.9–48.5]	0.04	46.5[38.1–52.1]	< 0.001
Left optic nerve max dose	42.4[33.5–50.2]	42.8[34–51]	0.001	44[35.5–53.5]	< 0.001
Right optic nerve max dose	41.8[33.8–49.2]	43.1[34.6–50.4]	0.001	44.7[36.4–54.8]	< 0.001
Left lens max dose	6.5[5.4–7.1]	6.8[5.5–7.6]	0.002	7.2[5.9–9.1]	0.001
Right lens max dose	6.4[5.4–6.8]	6.7[5.8–7]	0.002	7.1[6.1–7.3]	0.001
Left eye max dose	33.2[31.5–38.6]	34.7[33.2–39.7]	< 0.001	36.4[35.2–43.5]	< 0.001
Right eye max dose	32.9[30.7–37.5]	33.9[32.4–38.4]	< 0.001	35.8[34.6–41.8]	< 0.001
Left parotid mean dose	21.2[19.6–22.3]	24.3[21.8–26]	< 0.001	28.7[23.1–33.6]	< 0.001
Right parotid mean dose	22.3[20.1–23.1]	24.6[22.3–25.9]	< 0.001	27.9[24.6–34.7]	< 0.001
Left cochlea max dose	36.9[34.8–37.1]	39.5[36.2–40.5]	0.002	41.4[39.9–44.7]	0.001
Right cochlea max dose	35.7[34.4–36.7]	38.2[36.6–41.1]	0.001	40.9[38.7–43.5]	0.001
Oral cavity mean dose	29.5[26.5–28.4]	30.3[26.8–28.9]	0.21	31.1[26.9–29.4]	0.11

Dose evaluation for targets, conformity index, and homogeneity index

The target coverage evaluation could be calculated by determining the D5% and D95% values. For an ideal treatment plan, the values of D5% and D95% are equal to the prescribed dose (equal to 70 Gy in our study), indicating that 100% of the target is covered with the prescribed dose. In our study, the mean D95% in the iplan was 97% and significantly increased at Rplan1 with a mean value equal to 97.8%. At Rplan2, the mean D95% increased significantly compared with Rplan1, with a value of 98.5%. With the same pattern of D95%, the D5% increases significantly at Rplan1 and Rplan2 compared to iplan. The mean CI value at iplan was (0.72 ± 0.09), and then significantly decreased at Rplan1 (0.54 ± 0.15). In Rplan2, the CI value significantly reached (0.4 ± 0.15). Figure 3–14 shows the change in the conformity index during the RT course. The mean HI value increased significantly at Rplan1 compared to the iplan, where the mean value was (1.08 ± 0.03) and (1.1 ± 0.05) for iplan and Rplan1, respectively. The mean value of HI increased again at Rplan2 compared with that at Rplan1, with a mean value of (1.15 ± 0.03). The dosimetric changes that occur at the target are listed in Table 3.

Replanning (Adaptive Plans)

Dose evaluation for organs at risk using adaptive replanning

In this section, our strategy involved creating new VMAT plans after 10 and 20 treatment fractions, accounting for the (inter-fraction) anatomic changes, where the new plans were denoted as ARplan1 and ARplan2. The median maximum dose for the brainstem in the plan was 4920[4472–5322] cGy, which decreased significantly ($p < 0.001$) at ARplan1 to reach 4722[4375–5122] cGy. At ARplan2, the median maximum dose decreased again significantly ($p < 0.001$) compared to ARplan1 reaching 4631[4235–4990] cGy.

The spinal cord also showed a decrement in dose delivery, with a median maximum dose of 4015[3790–4222] cGy and significantly reached 3879[3688–4092] cGy at ARplan1. After 20 fractions, the dose was decreased again, with a median value of 3766[3552–3941] cGy.

For the Mandible, the median maximum dose was 6536[6311–7065] cGy, which then decreased significantly ($p < 0.001$) at ARplan1, reaching 6412[6188–6955]. The median maximum dose decreased insignificantly in ARplan2 compared to ARplan1, with a median maximum dose value of 6385[6141–6950] cGy. The optic chiasm substantially decreased the maximum dose ($p < 0.001$) after 10 and 20 treatment fractions, where the median maximum dose was 4250[3743–4788] cGy, 4120[3655–4492] cGy, and 4005[3520–4381] cGy for iplan, ARplan1, and ARplan2, respectively. Unlike the organs mentioned above, the parotid glands showed an increase in the mean dose at ARplan1 and ARplan2

compared to the iplan. For the left parotid gland, for instance, the median mean dose at the apex was 2121[1960–2228] cGy, which significantly increased to 2302[2030–2466] cGy at ARplan2, and increased again at ARplan2 to reach 2482[2212–2651] cGy. The doses received by the remaining OAR when using adaptive replanning are summarized in Table 4.

Dose evaluation for targets, conformity index, and homogeneity index using adaptive replanning

Using the replanning strategy, we were able to obtain stable coverage for the targets and ensure a homogeneous dose inside it, as we will see in the dosimetric evaluation of the target. The D5% was insignificantly changed during the VMAT course, where the mean D5% at iplan was 105 ± 0.02%, and 105.3 ± 0.014% for ARplan1, continuing with the same pattern at ARplan2 with a mean D5% value equal to 105.6 ± 0.02%. Additionally, for D95%, the value remained approximately consistent with adaptive replanning, where the mean D95% was 97 ± 0.07%, 97.1 ± 0.05%, and 96.9 ± 0.08% for iplan, ARplan1, and ARplan2, respectively. Because of steady target coverage with adaptive replanning, the HI and CI were almost steady. Table 5 presents the details of the target coverage, HI, and CI.

Table 3: Target coverage, conformity index, and homogeneity index at iplan, Rplan1, and Rplan2.

End Point (mean±SD)	iplan	Rplan1	P value (iplan vs. Rplan1)	Rplan2	P value (Rplan1 vs. Rplan2)
PTVp D5%	105 ± 0.02	107 ± 0.02	0.001	108 ± 0.02	0.004
PTVp D95%	97 ± 0.07	97.8 ± 0.06	0.007	98 ± 0.07	< 0.001
Conformity index	0.72 ± 0.09	0.54 ± 0.15	< 0.001	0.4 ± 0.15	< 0.001
Homogeneity index	1.08 ± 0.03	1.1 ± 0.05	0.003	1.15 ± 0.03	0.006

Table 4: Dose change for OAR at iplan, ARplan1, and ARplan2.

End Point median[25th, 75th] Gy	iplan	ARplan1	P value (iplan vs. ARplan1)	ARplan2	P value (ARplan1 vs. ARplan2)
Brainstem max dose	49.2[44.7–53.2]	47.2[43.8–53.2]	< 0.001	46.3[42.4–58.5]	< 0.001
Spinal cord max dose	40.2[34.9–42.2]	38.8[36.9–40.9]	< 0.001	37.7[35.5–39.4]	< 0.001
Mandible max dose	65.4[63.1–70.1]	64.4[61.9–69.6]	< 0.001	63.9[61.4–69.5]	0.62
Optic chiasm max dose	42.5[37.4–47.9]	41.2[36.6–44.9]	< 0.001	40.1[35.2–43.8]	< 0.001
Left optic nerve max dose	42.4[33.5–50.2]	41.6 [32.9–48.6]	0.025	40.8[31.4–47.2]	0.03
Right optic nerve max dose	41.8[33.8–49.2]	40.3[33–47.6]	0.027	38.9[30.9–45.3]	0.0024
Left lens max dose	6.5[5.4–7.1]	5.8[5.1–6.3]	0.015	5.6[4.9–6.3]	0.54
Right lens max dose	6.4[5.4–6.8]	5.7[5–6.6]	0.013	5.4[4.9–6.5]	0.52
Left eye max dose	33.2[31.5–38.6]	32.4[30.2–37.2]	0.026	31.5[29.5–36.6]	0.03
Right eye max dose	32.9[30.7–37.5]	31[29.5–36.3]	< 0.001	29.2[28.9–35.6]	0.001
Left parotid mean dose	21.2[19.6–22.3]	23[20.3–24.7]	< 0.001	24.8[23.1–33.6]	< 0.001
Right parotid mean dose	22.3[20.1–23.1]	23.9[21.5–24.9]	0.003	25[22.9–25.8]	< 0.001
Left cochlea max dose	36.9[34.8–37.1]	35.6[33.1–35.2]	< 0.001	32.2[32.6–33.1]	< 0.001
Right cochlea max dose	35.7[34.4–36.7]	33.9[33.1–34.8]	< 0.001	31.7[31.7–31.9]	< 0.001
Oral cavity mean dose	29.5[26.5–28.4]	29.3[26.2–28.5]	0.67	29.1[26–28.3]	0.58

Table 5: Target coverage, homogeneity, and conformity indices during adaptive replanning.

End Point (mean±SD)	iplan	ARplan1	P value (iplan vs. ARplan1)	ARplan2	P value (ARplan1 vs. ARplan2)
PTVp D5%	105 ± 0.02	107.3 ± 0.014	0.8	105.6 ± 0.02	0.78
PTVp D95%	97 ± 0.07	97.1 ± 0.05	0.78	96.9 ± 0.08	0.72
Conformity index	0.72 ± 0.09	0.7 ± 0.08	0.74	0.73	0.64
Homogeneity index	1.08 ± 0.03	1.09 ± 0.05	0.69	1.09 ± 0.04	0.74

DISCUSSION

In this study, all patients experienced significant weight loss during the course of RT, which is consistent with the results of previous studies.[19,20]

Weight loss can be related to the acute toxicity of radiation (and of course, from chemotherapy), compounded by concurrent chemoradiation administered to all patients.

In the context of HNC, the treatment volume is complex due to the proximity of several critical organs around the target, making complete protection difficult even with VMAT.

A study conducted by NAZRI et al. highlighted the multifactorial nature of weight loss in HNC patients, with factors such as chemotherapy, tumor staging, tumor site, and prescribed radiation dose laying significant roles.[21]

One potential contributor to weight loss is the radiation dose received by the parotid glands, which causes difficulty swallowing. In our study, tumor volume showed a significant decrease during the VMAT course. A study by Ishizawa et al. on HNC patients treated with RT concurrent with chemotherapy showed that 29% of patients showed more than 10% tumor shrinkage, with a median tumor shrinkage of approximately 5% of the initial tumor volume for all patients.[22]

Another study, which was conducted by Kulal et al. and included 40 patients with different HNC sites, also aligned with our research. All patients in Kulal et al. study received RT concurrent with chemotherapy and were re-imaged weekly with new contouring of the targets on the acquired CTs. The study showed a significant tumor volume reduction during treatment with a maximum reduction rate at weeks six and seven, where the mean tumor volume reduction rates were 15.4% ± 9% and 15% ± 8%, respectively.[23]

The present study also observed a significant decrease in the volume of the parotid glands during RT sessions, consistent with previous research.[24,25]

Sreejeev et al. conducted a study on HNC patients who underwent RT concurrent with chemotherapy, noting a significant weekly reduction in parotid gland volume, where the average parotid gland volume reduction (%) were 14.2%, 17.1%, 21.8%, 25.6%, 30%, and 32.1% from weeks 1–6, respectively.[26]

Furthermore, we observed that when we continued using the same plan during all treatment fractions, all organs showed a significant increase in dose delivery. The increase in dose to the spinal cord, brainstem, and optic structures could be related to the significant weight loss, where the reduction in patient weight leads to changes in the outer body contour and less attenuation of the beam's path. Consequently, the delivered dose to the organs exceeded the planned dose in the iplan. A study by Bhide et al. focused on patients with locally advanced HNC treated with IMRT. The study made use of newly acquired CT images at the second, third, fourth, and fifth week of treatment. The purpose of their study was to evaluate the anatomical and dosimetric changes during the RT course. One notable dosimetric observation was the significant increase in the spinal cord maximum dose after 20 and 25 treatment fractions when using the same treatment plan.[27]

Similarly, Beltran et al. conducted a study on 16 patients with HNC to evaluate the volumetric and dose changes to the target and OAR during the IMRT course, where the patients acquired new CT images at the 15th and 25th treatment sessions, revealing a substantial increase in the oral cavity mean dose, which is in agreement with our study.[28]

The parotid glands showed a significant increase in the mean dose after 10 and 20 treatment fractions, which could be due to weight loss, where the parotid glands faced a shift toward the high-dose region due to changes in the patient's external contour.

This result is in alignment with the research conducted by Lee et al. on HNC patients who were treated with the IMRT technique using helical tomotherapy; the parotid glands were contoured on the daily acquired megavoltage images, showing a significant increase in mean dose during treatment with an average increase of 10%.[29]

In a separate study by Castelli et al., 15 locally advanced HNC patients were treated with IMRT with weekly cone-beam CT acquisition. New plans were made based on the new CT images, and it was observed that the average overdose to the parotid glands without replanning was 4 Gy for 60% of the parotid glands.[30]

In contrast to our study which the target coverage of PTV_P ($D_{95\%}$) was increased after 10 and 20 sessions, Erick K. Hansen et al. conducted a dosimetric study for 13 HNC patients treated with IMRT with new CT during RT course and showed that the mean target coverage ($D_{95\%}$) was reduced by 0.8–6.3 Gy in 92% of the patients.[31]

Our study offers an explanation for the improvement in target coverage without the need for replanning: the tumor volume was reduced significantly during the VMAT course, which results in a decrease in the primary target volume, allowing for coverage of the entire target with the reference isodose (but the reference isodose will also cover nearby healthy tissues). Quantitatively, the target had a significant dose coverage (by improving the $D_{95\%}$), but qualitatively, the reference dose will fall in the healthy tissue area (which can be noted by the significant decrease in the CI value).

For the HI, the decrease in its value is due to the significant increase in the near maximum dose value of ($D_{5\%}$) for the target (which will produce hot spots inside the target). This increased dose heterogeneity inside the target will cause a significant decrease in the HI value. Our results align with a previous HNC study, which highlighted the generation of hot spots in the tumor due to anatomical changes during the RT course. Additionally, the study noted an increment in the dose received by organs when using the same plan for the entire RT course.[14]

The increment in the within the target without utilizing a replanning technique can be attributed to the patient's significant weight loss; therefore, the radiation beam had encountered less tissue on its way to the target (less than in the iplan). Upon implementing the adaptive replanning technique, it was observed that nearly all organs exhibited a significant decrease in dose delivery during the VMAT treatment sessions, which could be due to tumor volume reduction during the RT course. Consequently, the distance between the target and organs at risk increased, allowing for more precise sparing of surrounding organs without compromising target coverage. Our results align with a previous study on HNC patients treated with sequential IMRT, where a new plan was executed for those patients during the 17th fraction, which showed a significant decrease in the dose delivered to the brainstem, spinal cord, and optic chiasm.[32]

CONCLUSIONS

Our research suggests that individuals with locally advanced HNC undergoing modern RT techniques attain satisfactory results in terms of target coverage and sparing OAR. These results are attributed to the high dose-gradient difference of VMAT. However, substantial anatomical variations in patients during the RT course can impact notable alterations in the dosimetric outcomes of the VMAT plan. By iteratively adjusting the plan at specified intervals throughout the RT course, consistent (or better) dosimetric outcomes can be ensured. Patients with locally advanced HNC can be treated with modern RT techniques, with satisfactory results obtained in terms of target coverage and OAR regarding dose sparing.

REFERENCES

1. Lee SP, John MAS, Wong SG, Casciato DA. Head and neck cancers. In: Casciato DA, Territo MC, editors. Manual of clinical oncology. 7th ed. USA: Lippincott Williams & Wilkins; 2012. p. 171–202.
2. International Agency for Research on Cancer. Data visualization tools for exploring the global cancer burden in 2022 [Internet]. 2021 [cited 2023 Mar 8]. Available from: https://gco.iarc.fr/today/data/factsheets/populations/900-world-fact-sheets.pdf
3. Wong JW. Electronic Portal Imaging Devices (EPID). In: Brady LW, Yaeger TE, editors. Encyclopedia of radiation oncology. Berlin: Springer; 2013. Available from: https://doi.org/10.1007/978-3-540-85516-3_33
4. Ma DJ, Foote RL, Ang KK. Head and neck tumors: Overview. In: Gunderson LL, Tepper JE, editors. Clinical radiation oncology. 4th ed. Netherlands: Elsevier, Inc.; 2016. p. 591–9.
5. Jereczek-Fossa BA, Alterio D, Jassem J, Gibelli B, Tradati N, Orecchia R. Radiotherapy-induced thyroid disorders. Cancer Treat Rev. 2004;30(4):369–84. Available from: https://doi.org/10.1016/j.ctrv.2003.12.003
6. Pil J, Nevens D, Van der Vorst A, Gadan C, Nuyts S. The incidence of hypothyroidism after radiotherapy for head and neck cancer. B-ENT. 2016;12(4):257–62. Available from: https://pubmed.ncbi.nlm.nih.gov/29709128/
7. Ghosh A, Gupta S, Johny D, Bhosale VV, Negi MPS. A study to assess the dosimetric impact of the anatomical changes occurring in the parotid glands and tumour volume during intensity modulated radiotherapy using simultaneous integrated boost (IMRT-SIB) in head and neck squamous cell cancers. Cancer Med. 2021;10(15):5175–90.
8. Ho KF, Marchant T, Moore C, Webster G, Rowbottom C, Penington H, et al. Monitoring dosimetric impact of weight loss with kilovoltage (KV) cone beam CT (CBCT) during parotid-sparing IMRT and concurrent chemotherapy. Int J Radiat Oncol Biol Phys. 2012;82(3):e375–82.

9. Bhandari V, Patel P, Gurjar OP, Gupta, KL. Impact of repeat computerized tomography replans in the radiation therapy of head and neck cancers. J Med Phys. 2014;39(3):164–8.
10. Burela N, Soni TP, Patni N, Natarajan T. Adaptive intensity-modulated radiotherapy in head-and-neck cancer: A volumetric and dosimetric study. J Cancer Res Ther. 2019;15(3):533–8.
11. Buciuman N, Marcu LG. Adaptive radiotherapy in head and neck cancer using Volumetric Modulated Arc Therapy. J Pers Med. 2022 Apr 21;12(5):668.
12. Ding Y, Hazle JD, Mohamed AS, Frank SJ, Hobbs BP, Colen RR, et al. Intravoxel incoherent motion imaging kinetics during chemoradiotherapy for human papillomavirus-associated squamous cell carcinoma of the oropharynx: preliminary results from a prospective pilot study. NMR Biomed. 2015;28(12):1645–54.
13. Mohamed ASR, Bahig H, Aristophanous M, Blanchard P, Kamal M, Ding Y, et al. Prospective in silico study of the feasibility and dosimetric advantages of MRI-guided dose adaptation for human papillomavirus positive oropharyngeal cancer patients compared with standard IMRT. Clin Transl Radiat Oncol. 2018;11:11–8.
14. Morgan HE, Sher DJ. Adaptive radiotherapy for head and neck cancer. Cancers Head Neck. 2020 Jan 9;5:1.
15. Yen A, Shen C, Albuquerque K. The new kid on the block: Online adaptive radiotherapy in the treatment of gynecologic cancers. Curr Oncol. 2023;30(1):865–74.
16. Colvill E, Booth J, Nill S, Fast M, Bedford J, Oelfke U, et al. A dosimetric comparison of real-time adaptive and non-adaptive radiotherapy: A multi-institutional study encompassing robotic, gimbaled, multileaf collimator and couch tracking. Radiother Oncol. 2016;119(1):159–65.
17. Riet AV, Mac CA, Moerland MA, Elders LH, van de Zee W. A conformation number to quantify the degree of conformation brachytherapy and external beam irradiation: application in prostate. Int J Radiat Oncol Biol Phys. 1997;37(3):731–6.
18. Semerenko VA, Reitz B, Day E, Qi SX, Miften M, Li XA. Evaluation of a commercial biologically based IMRT treatment planning system. Med Phys. 2008;35(12):5851–60.
19. Lee S, Wang T, Chu P. Prediction of weight loss during and after radiotherapy in patients with head and neck cancer: A longitudinal study. Euro J Oncol Nurs. 2019;39: 98–104.
20. Ottosson S, Söderström K, Kjellén E, Nilsson P, Zackrisson B, Laurell G. Weight and body mass index in relation to irradiated volume and to overall survival on patients with oropharyngeal cancer: a retrospective cohort study. Radiat Oncol. 2014;9:160.
21. Nazari V, Pashaki AS, Hasanzadeh E. The reliable predictors of severe weight loss during the radiotherapy of head and neck cancer. Canc Treat Res Commu. 2021;26:100281.
22. Ishizawa M, Tanaka S, Takagi H, Kadoya N, Sato K, Umezawa R. Development of a prediction model for head and neck volume reduction by clinical factors, dose-volume histogram parameters and radiomics in head and neck cancer. J Radiat Res. 2023;64(5):738–794.
23. Kulal S, Vishwanathan B, SN G. A prospective study to assess for the prognostic value of tumor volume reduction rate in head and neck cancer, during definitive chemo-radiation in a tertiary care hospital. GSC Advanc Res Rev. 2023;15(3):273–86.
24. Yang H, Tu Y, Wang W, Hu W, Ding W, Yu C, *et al.* A comparison of anatomical and dosimetric variation in the 15 fractions, and between fractions 16 and 25, of intensity-modulated radiotherapy for nasopharyngeal carcinoma. J Appl Clin Med Phys. 2013;14(6):1–13.
25. Hunter KU, Fernandes LL, Vineberg KA, McShan D, Antonuk AE, Cornwall C, et al. Parotid glands dose-effect relationships based on their actually delivered doses: implication for adaptive replanning in radiation therapy of head-and-neck cancer. Int J Radiat Oncol Biol Phys. 2013;87(4):676–82.
26. Sreejeev AT, Joseph D, Krishnan AS, Ahuja R, Sikdar D, Raut S, et al. Serial assessment of parotid volume changes during radical chemotherapy of locally advanced head and neck cancer: its implications in practice of adaptive radiotherapy. Anna Oncol. 2020;31(6):1351.
27. Bhide AS, Davies M, Burke K, McNair HA, Hansen V, Barbachano Y, et al. Weekly volume and dosimetric changes during chemoradiotherapy with intensity-modulated radiation therapy for head and neck cancer: a prospective observational study. Int J Radiat Oncol Biol Phys. 2010;76(5):1360–8.
28. Beltran M, Ramos M, Rovira JJ, Perez-Hoyos S, Sancho M, Puertas E, et al. Dose variations in tumor volumes and organs at risk during IMRT for head-and-neck cancer. Int J Appl Clin Med Phys. 2012;13(6):101–11
29. Lee C, Langen KM, Lu W, Haimerl J, Schnarr E, Ruchala KJ, et al. Assessment of parotid gland dose changes during head and neck cancer radiotherapy using daily megavoltage computed tomography and deformable image registration. Int J Radiat Oncol Biol Phys. 2008;71(5):1563–71.
30. Castelli J, Simon A, Louvel G, Henry O, Chajon E, Nassef M, et al. Impact of head and neck cancer adaptive radiotherapy to spare the parotid glands and decrease the risk of xerostomia. Radiat Oncol. 2015;10:6.
31. Hansen EK, Bucci MK, Quivey JM, Weinberg V, Xia P. Repeat CT imaging and replanning during the course of IMRT for head-and-neck cancer. Int J Radiat Oncol Biol Phys. 2006;64(2):355–62.
32. Chitapanarux I, Chomprasert K, Nobnaop W, Wanwilairat S, Tharavichitkul E, Jakrabhandu S, et al. A dosimetric comparison of two-phase adaptive intensity-modulated radiotherapy for locally advanced nasopharyngeal cancer. J Radiat Res. 2015;56(3):529–38.